

FEEG6005 2024-25 Coursework 2

Student number: 36606782

Part 1

Q1

- 1) $Re = 305470$
- 2) I will be using a density of 1 kg/m^3 and a dynamic viscosity of $3.578e-6 \text{ kg/ms}$. The value for kinematic viscosity therefore will be the same ($3.578e-6$).

$$U_\infty = \frac{Re * v}{c} = \frac{305470 * 3.578e - 6}{1} = 1.09297166 \frac{m}{s} \quad (1)$$

$$BL \text{ thickness} = 0.37x \left(\frac{U_\infty * x}{v} \right)^{-0.2} = 0.37 * 1 * \left(\frac{1.09297166 * 1}{3.578e - 6} \right)^{-0.2} \quad (2)$$

Maximum BL Thickness = 0.02959429585 m

Q2

Table 1 Boundary conditions

	Inlet	Outlet	Airfoil	ProjAbove	ProjBelow	ProjUpstream	ProjWake
Boundary condition type	Velocities	Pressure Outlet	Wall	Interior	Interior	Interior	Interior

Q3

Using the following method, I calculated the friction velocity at the trailing edge:

$$U_* = \sqrt{0.0296 * \left(\frac{U_\infty * c}{v} \right)^{-0.2} * U_\infty^2} \quad (3)$$

Where U_∞ is the freestream velocity, v is the kinematic viscosity and c is the chord length. Using a standard value of $v=3.578e-6 \text{ kg/m-s}$, $c=1\text{m}$ and $Re=305470$:

$$U_* = \sqrt{0.0296 * \left(\frac{1.09297166 * 1}{3.578e - 6} \right)^{-0.2} * 1.09297166^2} = 0.0532 \quad (4)$$

Using the half height of the first cell as 0.0015m:

$$y_1^+ = \frac{y_1 U_*}{v} = \frac{0.0015 * 0.0532}{3.578e - 6} = 22.29506912 \quad (5)$$

y_1^+ at the trailing edge = 22.3

y_1^+ at the following chord length sections:

5% chord = 30.1
 10% chord = 28.1
 20% chord = 26.2
 40% chord = 24.4
 70% chord = 23.1

The greatest amount of shear stress will be at the leading edge and will decrease as a function of distance from this point. Since the friction velocity and y_1^+ are directly proportional, this explains the increase seen closer to the leading edge. These values are in the transition region (20-30) and so are not ideal for k-epsilon model due to the complex nature of flow in this region. Ideally, y_1^+ would range from 30 to 300 for the k-epsilon model to work ideally along the boundary layer as this is in the logarithmic region. However this model will still be accurate enough to perform at this marginal condition. To reduce this effect, the mesh resolution should be changed so that all values for y_1^+ are greater than 30. Alternatively, the values can be reduced to below 5 and a different turbulence model would have to be chosen.

Realizable k-epsilon model should be used for a industry project because it is still more suitable than the Spalart-Allmaras model. The Spalart-Allmaras model would perform even worse because it is used to resolve flow in the viscous sublayer with a $y_1^+ < 5$, whereas the values pertaining to this mesh are closer to the logarithmic region. Even though the y_1^+ values are in the transition region and so the velocity profile will be complex, the k-epsilon model will still be the most capable model for handling turbulence at the boundary layer.

Q4

The number of grid points in the boundary layer can be determined from the following calculation:

$$\text{no. of grid points} = \frac{\text{BL Thickness}}{\text{Cell height}} = \frac{0.03}{0.003} = 10 \quad (6)$$

Only ten grid points in the boundary layer is likely to be insufficient for resolving accurately. It is ideal to have more than ten grid points so this is the minimum amount needed for accurate results. Furthermore, the y_1^+ values are in the transition layer which adds to the likelihood of inaccuracy. Overall, the mesh resolution is too fine at the boundary layer whilst the amount of grid points in the boundary layer being too small.

Q5

Table 2 Pressure-Velocity coupling algorithm, spatial-discretisation schemes, detailed boundary conditions, and residuals to be achieved.

	Value	Reason
Pressure- Velocity coupling algorithm	SIMPLEC	Easier to achieve convergence than SIMPLE
Spatial- discretisation schemes	Least Squared Cell Based, Standard Pressure, Second Order Upwind Momentum & Turbulent Kinetic	Second Order Upwind schemes are better suited for this mesh resolution. If it was coarser, I would use first order.

	Energy & Turbulent Dissipation Rate	
Velocity BCs	1.09297166	Freestream velocity
Turbulence quantities at inlet	0.3% Intensity 1 Turbulent viscosity Ratio	Default values
Residuals (planned residuals to be achieved)	1e-5	Ideal level of accuracy

Q6

Table 3 C_l and C_d of the NACA 0012 Airfoil Section at a 6-degree angle of attack

	CFD	Expt. ($Re=2 \times 10^6$, Mach M=0.15, transition fixed at 5% chord) [1]	Expt. ($Re=2 \times 10^6$, Mach M=0.15, free transition) [1]
C_l	0.6044	0.6084	0.6250
C_d	0.0206	0.0134	0.0087

```
Console
 547 1.4707e-04 2.6900e-00 9.9934e-09 2.2067e-05 1.9023e-05 2.0553e-02 6.0431e-01 0:02:38 453
 548 1.2676e-04 2.6549e-08 9.6898e-09 1.4485e-05 1.5861e-05 2.0556e-02 6.0432e-01 0:02:06 452
 549 1.1012e-04 2.6194e-08 9.1134e-09 1.2424e-05 1.4791e-05 2.0554e-02 6.0433e-01 0:01:41 451
 550 1.0710e-04 2.5842e-08 8.7756e-09 1.1895e-05 1.3778e-05 2.0553e-02 6.0434e-01 0:01:20 450

  iter continuity x-velocity y-velocity      k     epsilon      cd      cl      time/iter
 551 9.9228e-05 2.5516e-08 8.5583e-09 1.1749e-05 1.3878e-05 2.0553e-02 6.0435e-01 0:01:04 449
! 551 solution is converged
Writing "| gzip -2cf > SolutionMonitor.gz"...
```

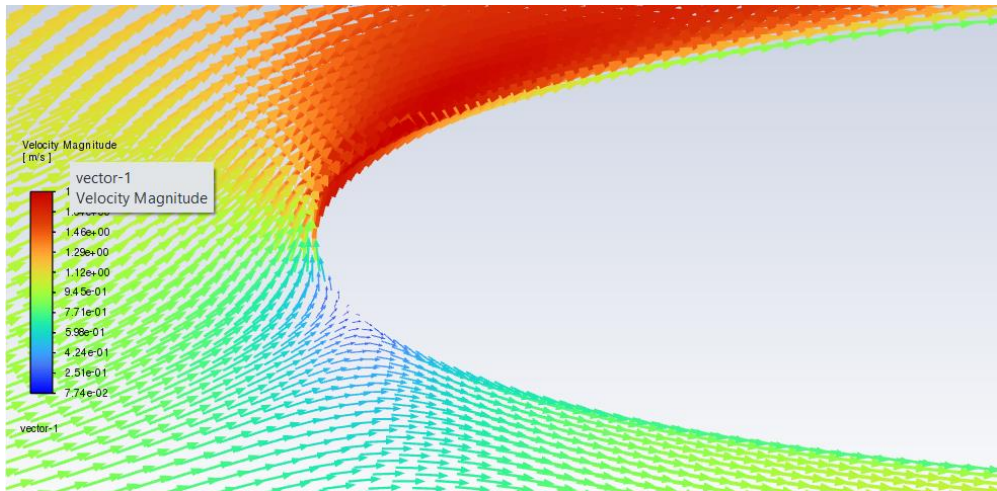
Fig.1. Results of solution converging in Ansys Fluent

The solution converges with residuals of 1e-4. These residuals were used because the solution failed to converge at the planned residual of 1e-5.

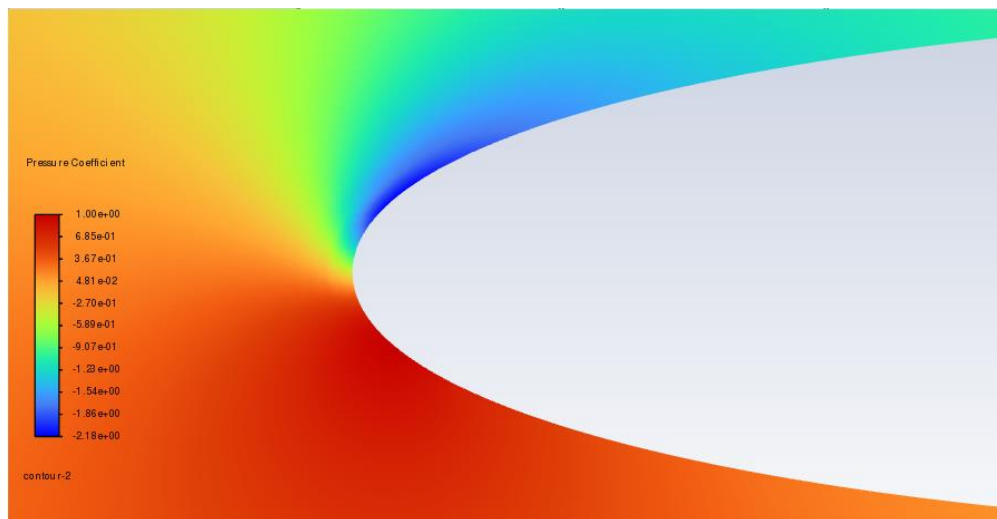
Firstly, the mesh used does not have a boundary layer to accommodate for the complex flow at the boundary of the airfoil. At this resolution, the flow is in the transition region and it is very difficult to solve the flow at the boundary. Also, the combination of using second order upwind schemes with a medium mesh may introduce spatial discretization errors if the mesh is not fine enough. Second-order schemes can suffer from truncations, caused by dispersion, when being used on a mesh with too low of a resolution.

The lift coefficient is many times more accurate than the drag coefficient. This may suggest that the simulation did not evaluate friction forces causing drag well enough. This is likely due to sub-optimal mesh size. Furthermore, it would be beneficial for a comparison using similar Reynolds numbers. The experimental data uses $Re=2e6$, whereas the Ansys simulation used $Re=305470$. These are significantly different and will affect the similarity of the comparative results.

Q7

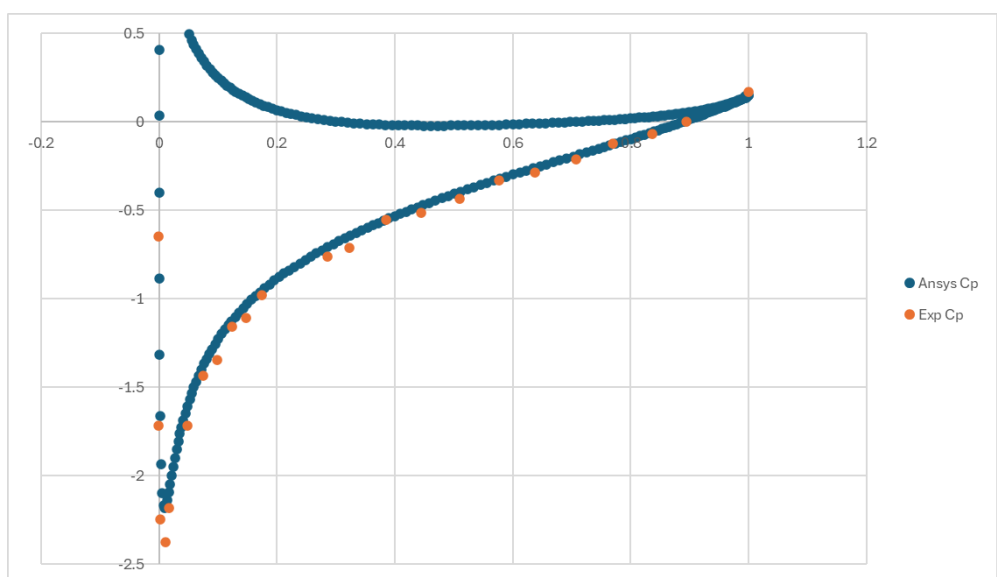


(a)



(b)

Fig. 2. (a) Velocity contours around airfoil in Ansys Fluent (b) Pressure coefficient around airfoil in Ansys Fluent



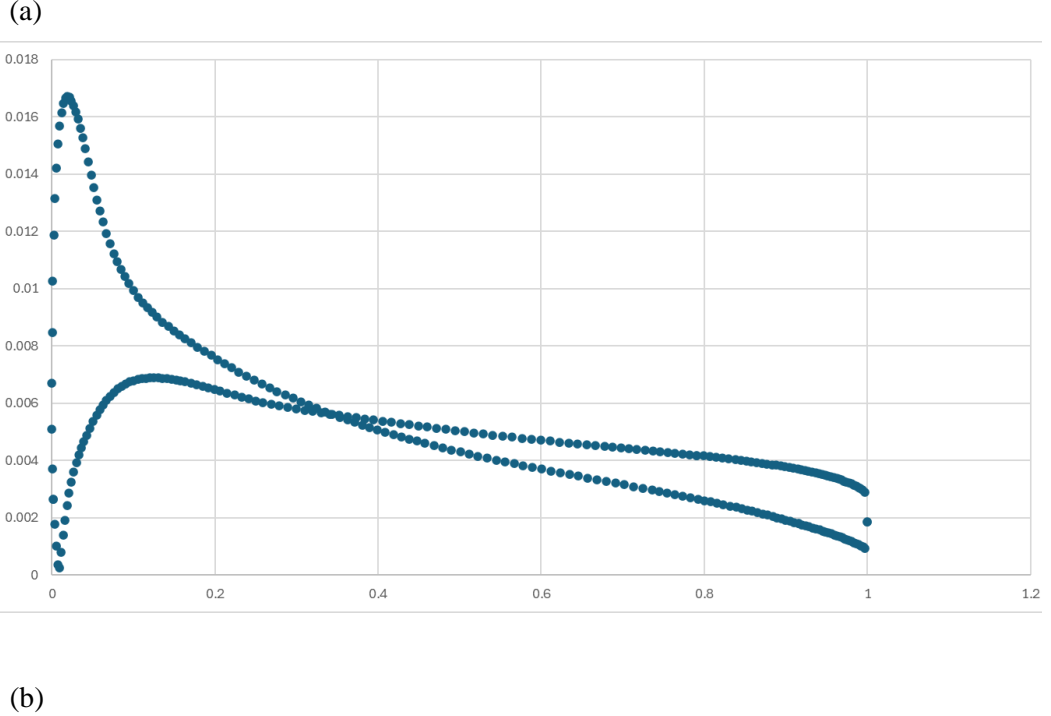


Fig.3. (a) A comparison of the C_p distribution against the experimental data; **(b)** C_f distribution

Fig. 2a presents the location of the stagnation point: the point of zero velocity of the airfoil. This should coincide with the leading edge adjusted for angle of attack. Fig. 2b shows that the pressure coefficient is 1 at the stagnation point. This is the expected value to see.

The magnitude of the skin friction coefficient reaches a maximum of ~ 0.017 , whereas the pressure coefficient reaches a maximum of 1 at a similar point in the plots. Fig 3a shows that the plot for pressure coefficient is fairly accurate overall with a slight deviation of ~ 0.2 at the maximum negative point on the plot.

I would like to have the solution converge at $1e-5$ to increase the confidence in the calculations of these values. However, I think they are overall fairly accurate. The y_1^+ values indicate that the flow over the airfoil at the boundary is complex. This means that even when using the k-epsilon model, errors will be introduced because the two equation model will not be sophisticated enough.

In general, the simulation for this medium mesh at moderate Reynolds number performed to a good standard even though the mesh seemed to be too coarse analytically. I would suggest that at more severe angles of attack, this simulation may not perform as well because I do not think it is set up well enough to handle more turbulent flows. A finer mesh would grant a higher likelihood for obtaining more accurate results when using more demanding input parameters because this current set up is not optimized.

Part 2

Q8

The refinement process involves refining the mesh within the boundary layer. The boundary layer thickness varies over the airfoil surface but is thickest at the trailing edge. At this point, there are ten cells within the boundary layer and so this number of cells will be refined all along the airfoil surface so that it is sufficiently encapsulated. There will be two layers of refinement; the layer closest to the wall being the finest. Therefore, the first five cells from the wall will be refined twice and the next five, only once. Refining once splits a cell into quarters: creating four cells with half the dimensions of the former cell.

Within Ansys Fluent, this is done via the manual adapt function. I set up two boundary cell registers with a distance of 10 cells from the wall. By performing this adapt function twice, it creates the desired mesh seen in fig 4.

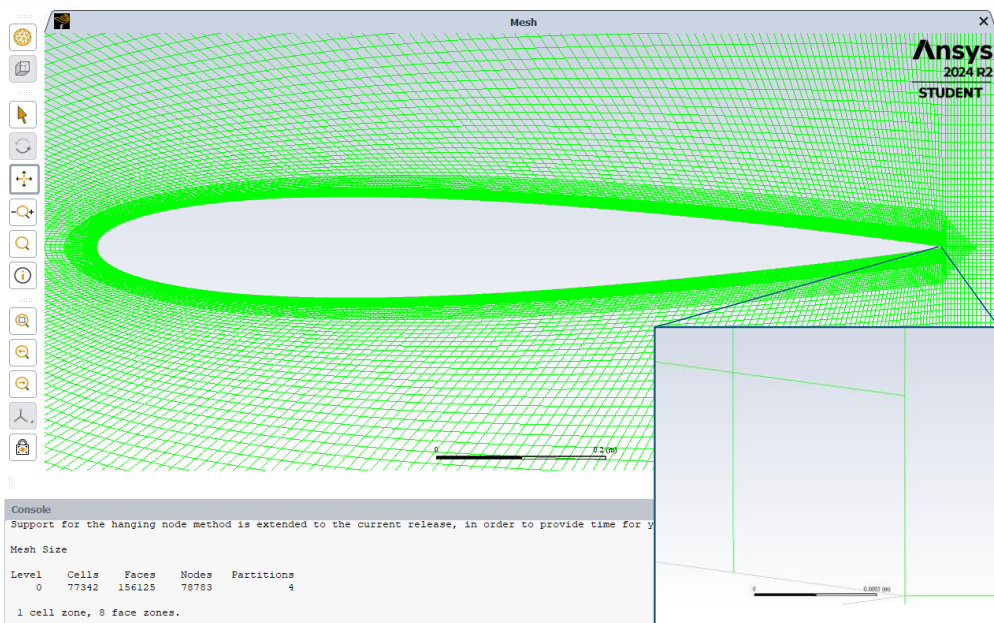


Fig. 4. Results from refining mesh in Ansys Fluent with zoom in of mesh at trailing edge

Using the ruler measure tool in Ansys Fluent, I determined the half height of the first cell at the wall of the trailing edge to be 0.0004m. Using this value, I calculated the analytical value for y_1^+ at the trailing edge:

$$y_1^+ = \frac{0.0004 * 0.0532}{3.578e6} = 5.945 \quad (7)$$

The process of refining the mesh aims to reduce the error in calculations in the most problematic regions. Namely this would be the region around the wall of the airfoil as the flow is unsteady and chaotic here (turbulent flow).

This y_1^+ is a lower value than the one pertaining to the previous, unrefined mesh and almost places the flow within the mesh at the wall within the viscous sublayer ($y_1^+ < 5$). At 5% of the chord length; $y_1^+ = 8$. This range of 5-8 is not ideal to fully place the flow within the viscous sublayer but aims to enable the simulation to more accurately solve turbulent flow at the wall. A different turbulence model, such as Spalart-Allmaras, should now handle flow at the wall of the airfoil more accurately than the previous model leading to an overall better simulation where forces on the wall

are key. Therefore, I will change the turbulence model to the Spalart-Allmaras and the turbulent viscosity ratio at the inlet and outlet boundary to be 1.

Q9

```
Console
1809 1.0237e-05 4.2411e-09 1.9923e-09 6.4338e-07 1.7441e-02 6.0009e-01 0:00:52 191
1810 1.0184e-05 4.2207e-09 1.9823e-09 6.3743e-07 1.7440e-02 6.0603e-01 0:00:41 190
1811 1.0113e-05 4.1970e-09 1.9715e-09 6.3167e-07 1.7440e-02 6.0604e-01 0:00:33 189
1812 1.0163e-05 4.1812e-09 1.9599e-09 6.2609e-07 1.7440e-02 6.0604e-01 0:00:26 188
1813 1.0069e-05 4.1575e-09 1.9486e-09 6.2065e-07 1.7440e-02 6.0604e-01 0:00:21 187
1814 9.9866e-06 4.1346e-09 1.9378e-09 6.1543e-07 1.7440e-02 6.0604e-01 0:00:17 186
! 1814 solution is converged
Writing "| gzip -2cf > SolutionMonitor.gz"...
Writing temporary file C:\Users\User\AppData\Local\Temp\flntgz-85968 ...

Fig. 5. Results from simulation run using refined mesh
```

Using the refined mesh and the changes detailed above, the simulation was able to converge with residuals of 1e-5.

Table 4 A comparison of the lift coefficient Cl , drag coefficient Cd of the two resolutions

	CFD with medium resolution	CFD with refined resolution
Cl	0.6044	0.6060
Cd	0.0206	0.0174

The coefficient of lift reaches a slightly higher level of accuracy, reducing error of 0.004 to 0.0024, with regards to the experimental value of 0.6084. That is a 40% reduction in error.

The coefficient of drag is much improved by reducing error from 0.0072 to 0.0040, with regards to the experimental value of 0.0134. This is a 55% reduction in error. This improvement indicates that the frictional forces at the boundary are being solved better which is likely caused by the change in mesh and suitable turbulence model.

Q10

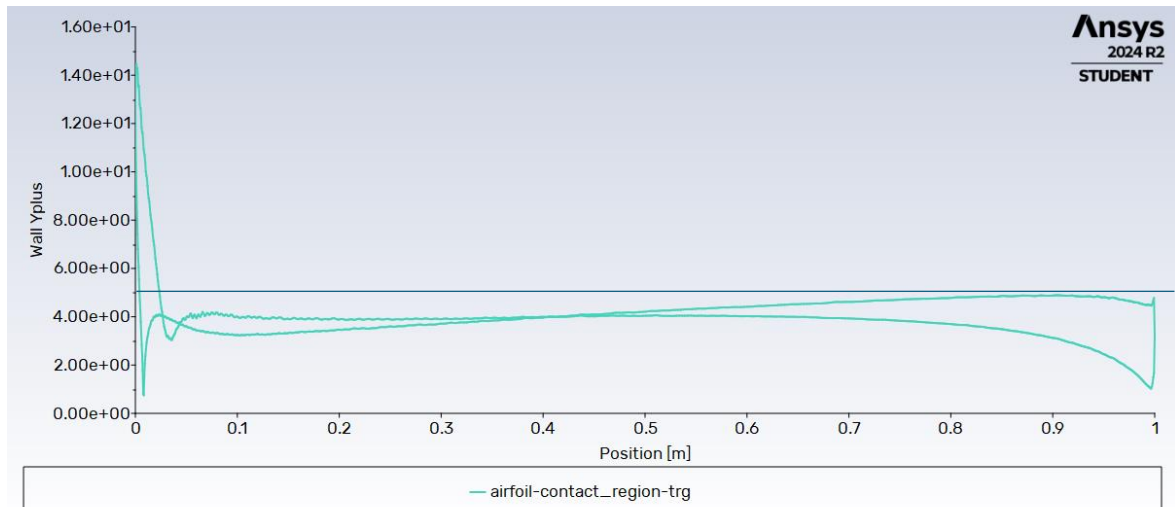


Fig. 6. Plot of y_1^+ over airfoil surface with line at $y_1^+ = 5$

The analytical method did predict a range of ~ 8 at 5% of chord, increasing to ~ 5 at 100% chord. As seen in Fig. 6, y_1^+ decreases from ~ 14 to 5 within the 2.5% of the chord length. This is reasonable as the friction velocity will be at its largest here but does stay within the viscous sublayer ($y_1^+ < 5$) for the remainder of the length. The chosen turbulence model (Spalart-Allmaras) works ideally at these values and so this numerical evidence of y_1^+ values further supports the use of Spalart-Allmaras (SA), in this application.

Q11

I will be using the refined mesh along with the SA turbulence model as it has shown to be more competent when dealing with the aerodynamic forces at the wall by reaching more accurate values for coefficients and is able converge at 1e-5 residuals.

Further simulations were carried out for the following angles of attack $\alpha = -12^\circ, -10^\circ, -8^\circ, -6^\circ, -4^\circ, -2^\circ, 2^\circ, 4^\circ, 8^\circ, 10^\circ, 12^\circ$. Residuals of 1e-5 were obtained for every simulation, although the number of iterations were increased to 2500 for 12 and 10 degrees.

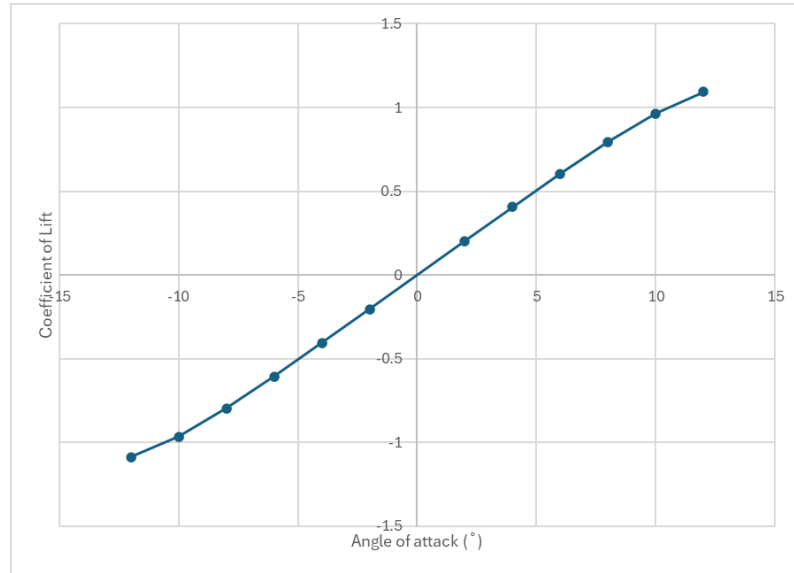


Fig. 7. Cl vs Angle of attack

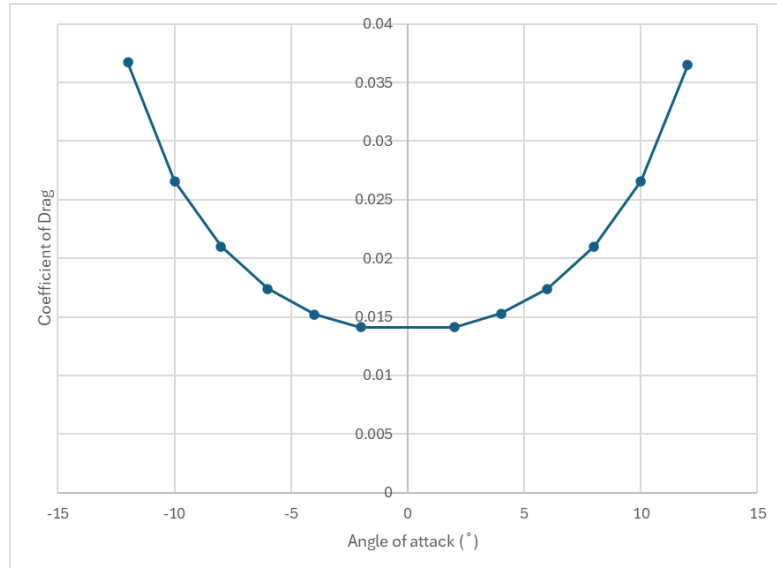


Fig. 8. Cd vs Angle of attack

The gradient of the linear region of the slope shown in Fig. 7 is roughly $\frac{dCl}{d\alpha} = \frac{1}{10} = 0.10$ between the points of -5 and 5 degrees. The line has a noticeably unvarying gradient between these points and C_p increases from -0.5 to 0.5. According to thin airfoil theory, the gradient can be estimated to be $\frac{dCl}{d\alpha} = \frac{2\pi^2}{180} \approx 0.1097$. The agreement between this estimation and my value calculated from simulations is good, with only a difference of 9.7%.

Table 5 Comparison of positive and negative coefficient of lift values

Angle of Attack ($^\circ$)	Positive Cl	Negative Cl	Absolute difference
12	1.0939	-1.0881	0.0058
10	0.9638	-0.964	0.0002
8	0.7947	-0.7948	1E-04
6	0.606	-0.6061	1E-04
4	0.4075	-0.4059	0.0016
2	0.2037	-0.2039	0.0002

The average of difference between positive and negative values is 0.0013. The largest error coming from the ± 12 degree simulations could be due to the flow becoming more turbulent and chaotic at this higher angle of attack which may introduce more errors in calculation from the turbulence model.

Additional angles of 13, 14 and 16 were simulated and the point of maximum Cl estimated from the results. The near stall angle associated with the highest coefficient of lift can be determined from Fig. 9. The near stall angle is estimated to be 13.5 degrees from the Fig. 9. As the angle increased, the simulation struggled to converge to the residual of 1e-5. However, all simulations managed to successfully converge at 1e-5 residuals. I expect the increased amount of friction and drag introduced from the steeper angle of attack causes the simulation to take longer to converge.

From the plot shown on Fig 9, I estimated the maximum Cl to be 1.14 at a near stall angle of 13.5 degrees. Running a simulation at -13.5 degrees yielded a Cl of -1.1281. This discrepancy is about 0.012; about 1% of the absolute value. This error is small enough to grant a good level of confidence because the average error value for all the previous points was 0.0013.

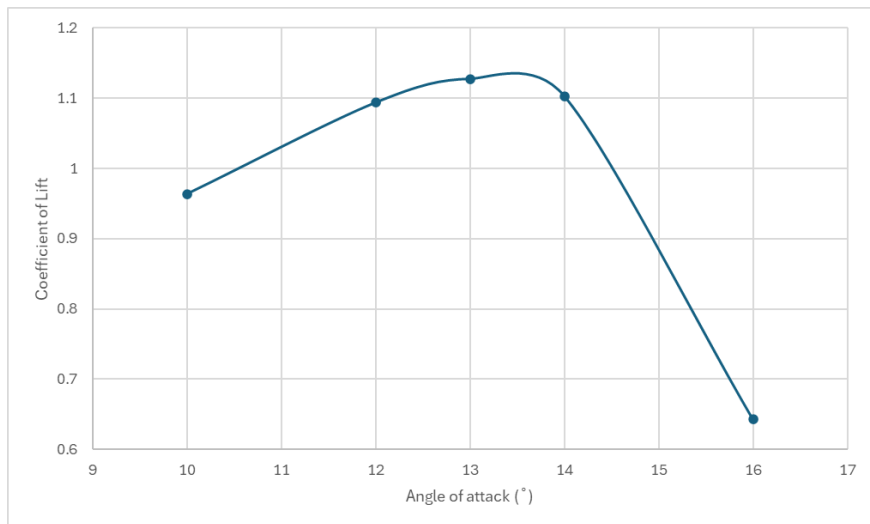


Fig. 9. Plot of high angles of attack around near stall angle

Q12

By keeping the Reynolds number the same and multiplying the kinematic viscosity by 6 and freestream velocity by 2, the chord length triples. So I have scaled up the imported structured mesh sizing by a factor of 3.

$$Re \frac{6\nu}{2U_\infty} = 305470 * \frac{6 * 3.578e - 6}{2 * 1.09297166} = c = 3 \quad (8)$$

The boundary layer thickness has been tripled as well but since the mesh sizing has tripled as well, the analytical y_1^+ value stays about the same. Furthermore, the turbulence quantities at the inlet and outlet boundaries need to change. As I am using the SA turbulence model, the turbulent viscosity ratio is the only parameter available. I changed this from 1 to 6 to accommodate for the change in viscosity.

Table 6 A list of the changes of settings compared to Question 8.

	<i>Q8 settings</i>	<i>Q12 settings</i>
Turbulent viscosity ratio	1	6
Dynamic Viscosity	$3.578e-6$	$2.1468e-5$
Reference pressure location	-5m	-15m
Inlet x-velocity	1.0870	2.1740
Inlet y-velocity	0.1142	0.2285
Cd force vector	X=1.0870 Y=0.1142	X=2.1740 Y=0.2285
Cl force vector	X=-0.1142 Y=1.0870	X=-0.2285 Y=2.1740
Reference Area	$1m^2$	$3m^2$

Q13

Achieved residuals of 1e-5.

Table 7 A comparison of the lift coefficient Cl, drag coefficient Cd of the two cases

	<i>Q9</i>	<i>Q13</i>
Cl	0.6060	0.6058
Cd	0.0174	0.0177

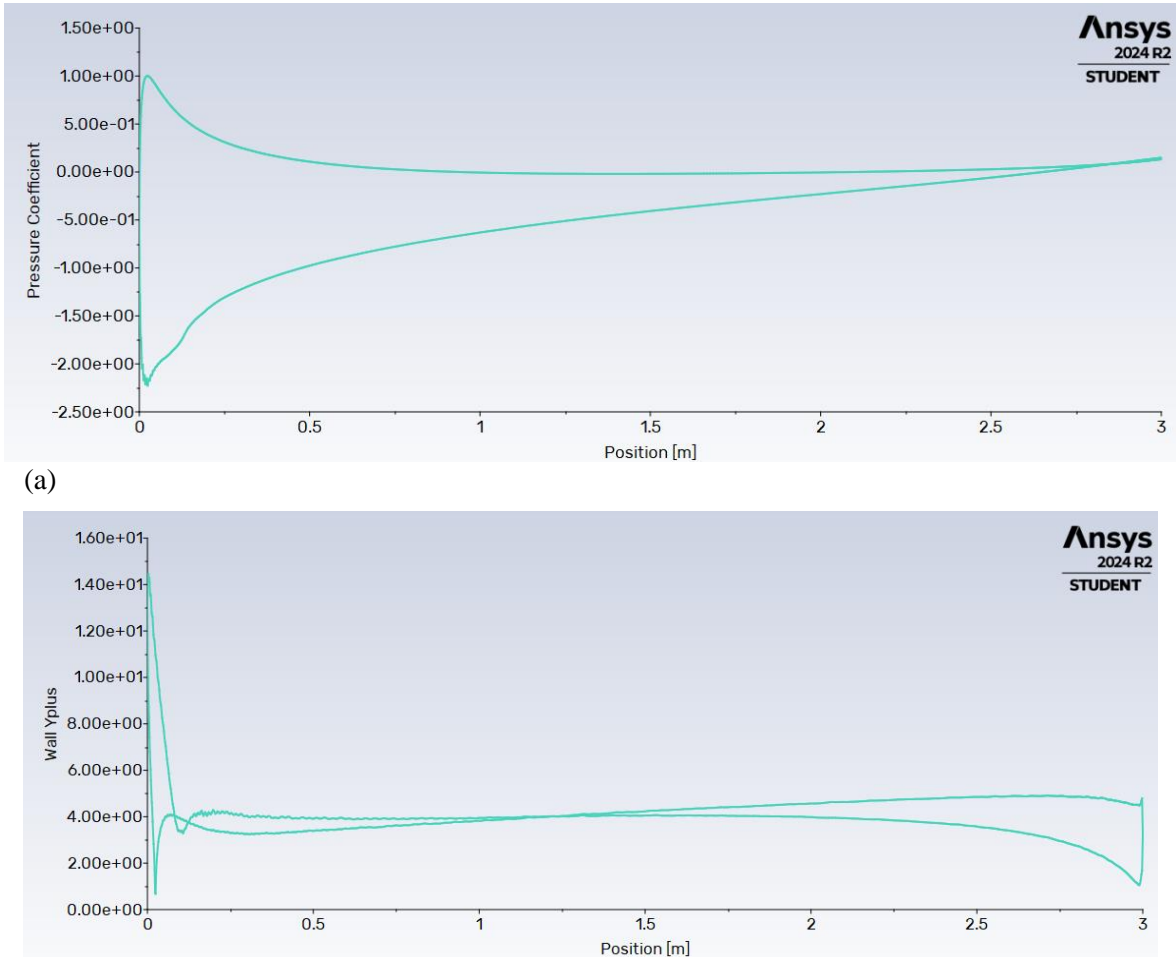


Fig. 10. a) Pressure coefficient over airfoil surface **b)** y_1^+ values over airfoil surface

According to Reynolds law of similarity, the flows between two simulations using the same Reynolds number should behave in an identical manner. So it would be reasonable to predict that in this situation, the flows should be identical when compared to Q9 results. Also, the geometry of the airfoil has been kept the same as both y and x dimensions of the mesh have been scaled up by 3, so there should be little difference between the two simulations. Fortunately, the results of this simulation are very similar to the results from Q9. The plots of y_1^+ and C_p are almost identical to the plots in Q9, as expected. Furthermore, as the coefficients of lift and drag are dimensionless, and so do not scale with model/airfoil size and are expected to stay the same. Changing the reference value for area to 3 was critical in this particular simulation because otherwise the coefficient would scale with its associated force, causing the coefficients to triple. Changing the reference value for area to 3 negated this potential issue. Overall, these results are in line with theoretical predictions, such as Reynolds law of similarity.

Q14

The Reynolds number for this new simulation will be $3.0547e6$. This is ten times the previous number and the freestream velocity is multiplied by ten to match this change since the chord length and kinematic viscosity are unchanged. Using the same methods outlined in question 2, I have estimated the maximum boundary layer thickness:

$$BL = 0.37 * \left(\frac{10.9297166 * 1}{3.578e-6} \right)^{-0.2} = 0.0187m \quad (9)$$

This reflects the boundary layer at the trailing edge of the airfoil. As the cell height is 0.003, there will be six grid points within the boundary layer.

Next, I have calculated the friction velocity at this point:

$$U_* = \sqrt{0.0296 * \left(\frac{10.9297166 * 1}{3.578e - 6} \right)^{-0.2} * 10.9297166^2} = 0.4224 \quad (10)$$

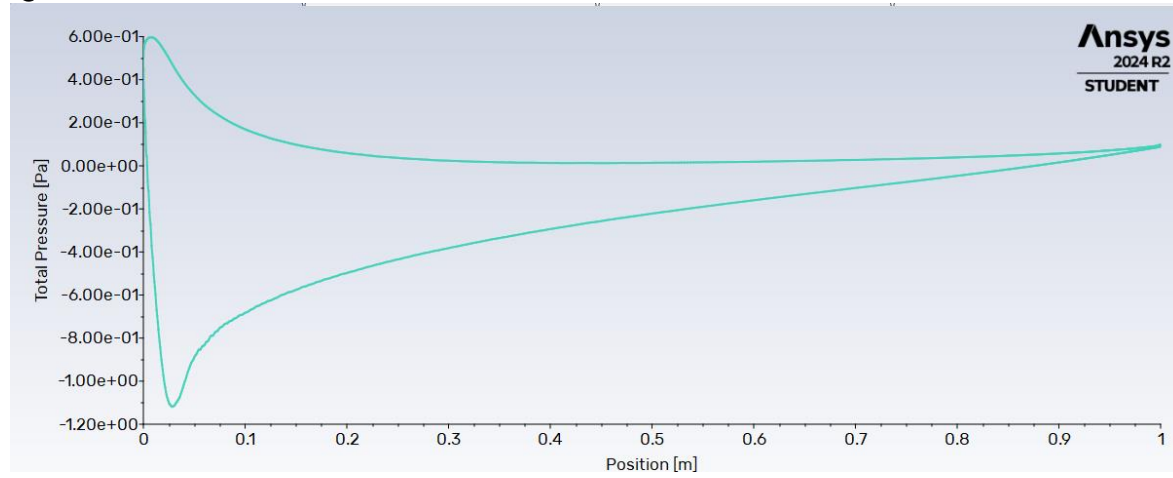
Using a half height of 0.0015m from the original mesh, the y_1^+ value is estimated by:

$$y_1^+ = \frac{0.0015 * 0.4224}{3.578e - 6} = 177 \quad (11)$$

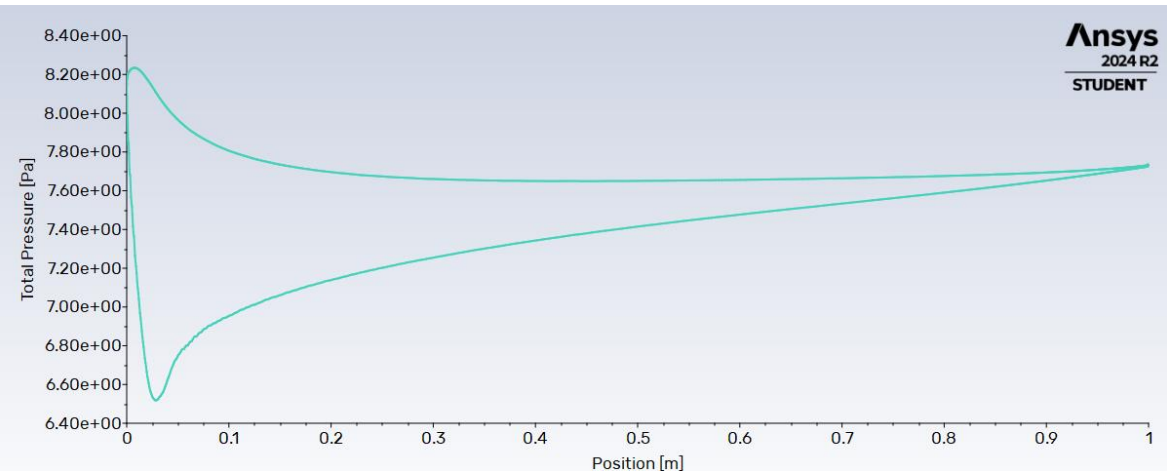
This would put the flow at the boundary into the logarithmic layer as it is between 30 and 300. To put it in the viscous sublayer; y_1^+ must be reduced to below 5 but ideally around 1. To achieve this, the mesh around the boundary must be refined to a point where the cell half height is below 0.000042. If the cells are halved in size six times, this will bring the cell height to 0.0000234, bringing the y_1^+ well within the viscous sub layer with a value of approx. 2.8. By refining the mesh in this way, the total number of cells in the mesh will increase significantly. Assuming another double layer of refinement, I estimate the number of cells to increase from 50000 to approx. 12 million.

I estimated there to be 400 cells lining the wall of the airfoil. There will be two layers of refinement; one where the cells have been halved five times and six on the other closest to the wall. Each cell in the first layer will become 4096 cells and so there will be $400 * 6 * 4096 = 9.83e6$ cells in the first layer. Using the same logic, the second layer of the refined mesh would be populated by $2.46e6$ cells. Obviously, this is a dramatic increase from the original 50000 cells and so computational power would have to significantly increased to cope.

Q15

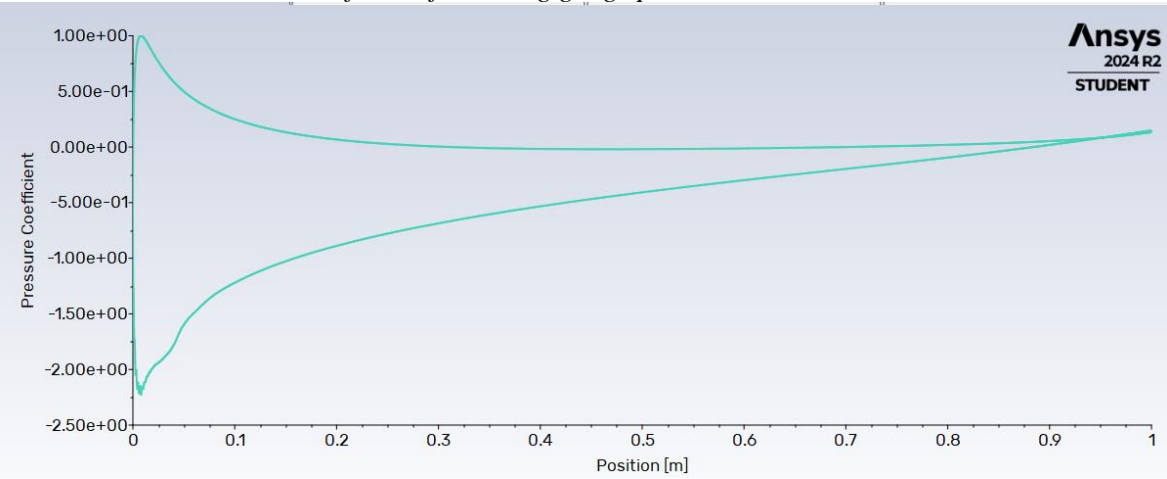


(a)

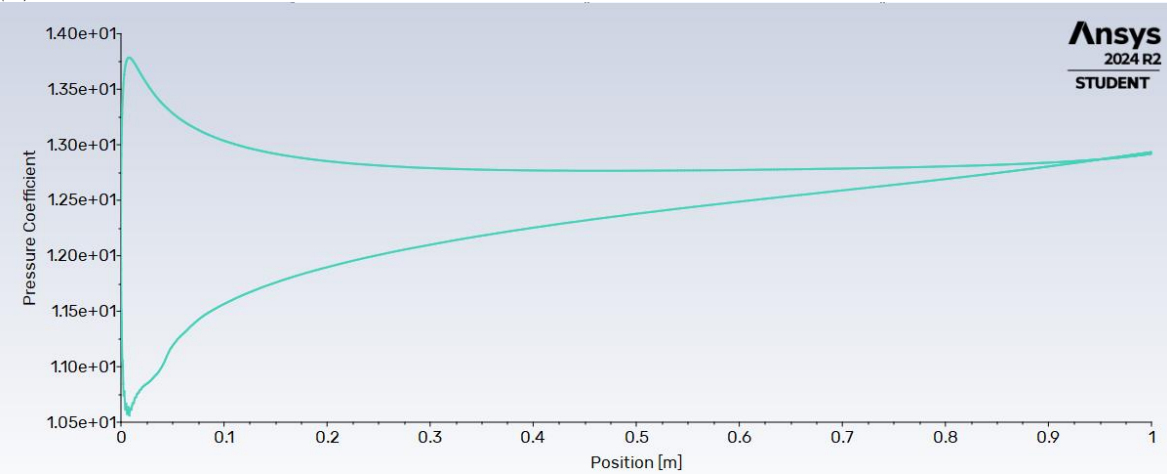


(b)

Fig. 11. a) Total pressure over airfoil surface using gauge pressure=0 b) Total pressure over airfoil surface using gauge pressure=7.63675



(a)



(b)

Fig. 12. a) Pressure coefficient over airfoil surface using gauge pressure=0 b) Pressure coefficient over airfoil surface using gauge pressure=7.63675

Table 8 A comparison of the lift coefficient C_l , drag coefficient C_d of the two gauge pressures

	Gauge Pressure=0	Gauge Pressure=7.63675
C_l	0.6060	0.6060
C_d	0.0174	0.0174

Even though the pressures measured over the airfoil increased when gauge pressure was increased to 7.6, the coefficients of lift and drag were unchanged. The values are identical in both cases.

Q16

The gauge pressure changing from 0 to 7.6 at the inlet and outlet boundaries does not change the overall pressure gradient of the fluid inside the domain. The SIMPLEC pressure-velocity coupling algorithm used in the simulation only considers the pressure gradient and so will be unaffected by this change.

The gauge pressure has been increased to simulate the lower atmospheric pressure within a Martian environment. Even though this pressure has changed, the coefficients of lift and drag remain the same as when simulating for an Earth environment because the pressure gradient has been unchanged. The pressure gradient is the factor that the RANS equations consider to solve the flow. Values for absolute pressures are not taken account when solving incompressible flows. The pressure gradient is the driving force for the fluid and does not change across the domain, when increasing gauge pressure, meaning that there will be no change in the general behaviour of the fluid.